PHYSICAL REVIEW B VOLUME 2, NUMBER 6 15 SEPTEMBER 1970

Influence of Hydrostatic Pressure and Temperature on the Deep Donor Levels of Sulfur in Silicon†

D. L. Camphausen,* H. M. James, and R. J. Sladek
Department of Physics, Purdue University, Lafayette, Indiana 47907
(Received 16 February 1970)

The Hall effect and resistivity of silicon doped with sulfur have been measured as a function of temperature in the range between 300 K and temperatures as low as 50 K (the latter depending on the sample in question) and as a function of hydrostatic pressure up to 8 kbar at various temperatures in this range. From the Hall-effect data, three of the four known levels of sulfur in silicon were found to have ionization energies in meV as follows:

A: $(105 \pm 15) - (0.22 \pm 0.03)P + (0.25 \pm 0.05)T$,
B: $(190 \pm 20) - (0.55 \pm 0.05)P + (0.057 \pm 0.012)T$,
C: $(360 \pm 30) - (1.1 + 0.1)P - (0.61 \pm 0.12)T$,

where P is in kbar and T is in K. The temperature dependence of the ionization energies may be due to electron-phonon interaction, but neither the sign nor magnitude of the effect has been calculated theoretically. With changing pressure, each level shifts with respect to both conduction- and valence-band edges at a rate that decreases with its distance from that band edge. This "rubber-band effect" is discussed qualitatively. A group-theoretical analysis is made of the Bloch waves that can appear in expansions of localized-impurity wave functions of various symmetries. This provides a basis for drawing some inferences concerning the symmetry of impurity centers from the presence or absence of the rubber-band effect. The observed effects are consistent with the idea that the D center is a substitutional S^+ at a T_d site; that the C center is an S_2^+-center with D_{3d} symmetry; that the B center is the neutral version of the C center; and that the A center is not simply the neutral version of the D center, but may represent as well the effects of interstitial sulfur at D_{3d} sites. With no applied pressure, the Hall mobility was found to have a magnitude and temperature dependence in samples prepared from undoped silicon different from that in samples prepared from boron-doped silicon. A quantitative explanation of the mobility is lacking, but it appears that scattering by agglomerations of sulfur might be important, in addition to scattering by lattice vibrations, ionized impurities, and neutral impurities. The pressure dependence of the Hall mobility is very small and can be attributed, at least in part, to the decrease of effective mass with increasing pressure.

I. INTRODUCTION

Donor impurities in a semiconductor are commonly classified as "shallow" or "deep," according to the depth of their ground-state levels below the conduction-band edge. Herein the term "deep" donor will denote a donor impurity with ground-state energy much lower than that predicted by the effective-mass approximation (EMA) of Kohn and Luttinger.[1]

There is a wealth of information on the energy and charge states of many deep donors in semiconductors. There are also some electron spin resonance and ENDOR measurements that give atomic configuration information and some crude evidence on the nature of the wave functions, respectively.[2] The understanding of deep donors is, however, still rather poor: Little is known about the details of their wave functions, and a reliable method for calculation of their energy levels is lacking. Several attempts to explain the energies of deep levels in semiconductors have been reviewed by one of the authors (DLC).[3]

When hydrostatic pressure is applied to a semiconductor, the various electronic energy bands shift relative to one another. These shifts have been investigated[4,5] extensively. Shallow donors in Ge and Si have been found to follow the conduction-band minima with which they are "associated" as the minima shift with pressure.[6] Any displacement of the ground-state energy level relative to these minima can be explained in terms of changes in the effective mass and the dielectric constant as the pressure is increased.

In contrast to shallow donor levels, deep levels in Ge and Si move toward or away from the nearest conduction-band edge with a variety of rates as pressure is applied, usually moving at a higher rate relative to the conduction-band edge than to the valence-band edge.[7]

In several III-V and II-VI compounds recently reviewed by Paul,[7] there exist energy levels that appear to be shallow, or even degenerate with the bottom of the conduction band, but which do not fol-

low the lowest conduction band when pressure is applied. The pressure coefficient of their separation from this band may be as large as the pressure coefficient of the whole width of the forbidden band. Such shallow levels tend to occur when there are several symmetry-inequivalent conduction bands with extrema near the forbidden band. Paul has suggested that the impurity states may be associated with any one (or several) of these conduction bands, and not necessarily with the lowest of them. To understand the pressure shifts in such cases, one must take account of the relation of the impurity states to all nearby conduction bands.

Impurity states associated with higher-lying conduction-band minima have been investigated theoretically by Peterson, by Kaplan, and by Shimizu.[8] Their theories characterize the impurity states that might occur for various band structures of the host semiconductor. These theories do not, however, indicate how deep an impurity potential must be in order to produce localized states, nor do they agree on the lifetimes of virtual states.

Donor levels are currently divided into three categories by reference to their pressure coefficients. First, there are shallow donor levels, almost "fixed" to the lowest conduction-band minima, and shifting with respect to them only to the extent accountable for by changes in the electronic effective mass m^* and the dielectric constant κ. Second, there are levels deep in the gap, sometimes exhibiting both donor and acceptor characteristics (as with Au in Ge), which are somehow fixed to the valence band. Third, there are levels associated with conduction-band edges other than the lowest, which shift together with these edges. One must also expect that there will be impurity states that are associated with no single energy band, and which exhibit an intermediate behavior. An appropriate theory of donor states should be able to predict the location of the levels relative to band extrema as a function of lattice dilatation and should also provide information about the wave functions of these states. Since such theory is lacking, experiments on impurity levels and their pressure dependences need to be continued in the hope of establishing a pattern to aid the construction of a theory.

II. SULFUR IN SILICON

Silicon doped with sulfur was chosen for this investigation because of the availability of detailed information about the band structure of silicon and because previous work had already provided some information about the deep donor levels that sulfur introduces into silicon. This includes data by Krag *et al.*[9] on the infrared excitation spectra and their behavior under uniaxial stress (to determine site symmetry) and ESR and ENDOR measurements by Ludwig,[10] which give information about the atomic configuration and about the impurity wave function. Sulfur goes into silicon both as atomic sulfur S and as a complex S_2. Krag *et al.* determined ground-state energies of four sulfur levels, which they designated as *A*, *B*, *C*, and *D* (see Fig. 1). They concluded that the *A* and *B* centers are neutral, whereas the *C* and *D* centers are singly charged; that the *A*, *B*, and *C* centers do not have tetrahedral symmetry; and that the *B* center has C_{3v} or D_{3d} site symmetry, with a trigonal axis along one of the ⟨111⟩ crystal axes. Figure 1 summarizes this information, together with conclusions about the *C* and *D* centers drawn by Ludwig.

The ESR data of Ludwig[10] on *D* centers produced by doping silicon with sulfur enriched in S^{33} showed that these centers consist of isolated sulfurs, singly ionized. The fact that the *g* factor of the *D* center is close to 2 supports this conclusion and indicates that the ground state (*D* level) is orbitally nondegenerate. Furthermore, Ludwig's detailed ENDOR study of the hyperfine interaction of the *D* center with the neighboring Si^{29} nuclei indicates that the S^+ ion is isolated in the lattice, with no compensating charge nearby, and that it is in a site of T_d symmetry. He was not, however, able to conclude with certainty whether the S^+ center occupies a substitutional T_d site or an interstitial site with a similar arrangement of neighbors. His observed hyperfine interaction constants were inconsistent with a Kohn-Luttinger wave function derived using the effective-mass approximation. He concluded that the simple effective-mass treatment failed to account for the amplitude of the wave functions at nearby lattice sites and that the contributions to the wave function from other parts of the band structure (primarily the Δ_2' edge) might be important.

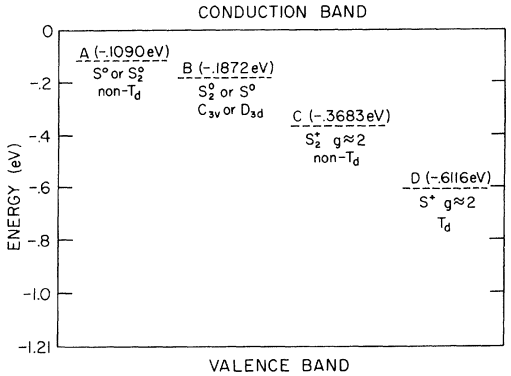

FIG. 1. Characteristics of sulfur energy levels in silicon. The information is taken from Krag *et al.*, Ref. 9, and Ludwig, Ref. 10.

It should, however, be noted that in this calculation Ludwig used an incorrect ionization energy (0.52 eV) for the S^+ level.[11]

Ludwig[10] studied the *C* center using samples in which Carlson *et al.*[12] had found the 0.37-eV level electrically and also samples in which Krag and Zeiger[13] had studied the *C* center optically. His ESR intensities in samples enriched in S^{33} showed that the *C* center consists of two *equivalent* sulfurs – a near pair of substitutional sulfurs, or two sulfurs in equivalent interstitial sites. Since the center is clearly singly ionized, it may thus be referred to as an S_2^+ center. The fact that the *g* factor is very close to 2 indicates that there is no orbital degeneracy in the S_2^+ ground state.

The observations of Krag *et al.* do not determine the exact nature of the *B* center. If its symmetry is C_{3v}, it is probably not a single sulfur atom in a substitutional site, but rather a pair of sulfur atoms. If its symmetry is D_{3d}, it may be a single interstitial sulfur atom, as will be discussed in Sec. V.

An energetic argument[3] can be given to support the idea that the *A* center is a pair of sulfur atoms, the neutral version of the *C* center, and the *B* center is a single sulfur atom, the neutral version of the *D* center. This is based on a comparison of the ionization energies of the *A*, *B*, *C*, and *D* centers with those of H_2, He, H_2^+, and He^+. The conclusion is, however, open to some doubt, since the factors that determine the energy of binding of electrons to S atoms in a crystal matrix are not entirely parallel to those that determine the energy of binding of electrons to point changes *in vacuo*. It is possible that two sulfur atoms could form a compact molecule in an interstitial site in the lattice, with a higher ionization energy than a single neutral sulfur, and that the *B* center would thus be an S_2 center and the *A* center an S center. Indeed, the outer electron is more strongly bound in the free molecule of diatomic sulfur than it is in the free sulfur atom.[14] There seems at present to be no compelling argument to indicate the nature of the sulfur configurations in the *A* and *B* centers.

In this work it was our intention to dope with sulfur silicon samples which had appropriate concentrations of acceptors and shallow donors so that only one level would be ionizing in a given sample over the whole temperature range of interest (50–300 K). This was found to be impossible in some cases, since the *B*(0.19-eV) level and *A*(0.10-eV) level could exist in the same sample, and their energies are quite close. However, from the Hall-effect–versus–temperature data it could be determined which level was ionizing in a particular temperature interval. The concentration and ionization energy of each type of deep donor level and the difference between the concentrations of acceptors and of shallower donors were determined by least-squares fitting of suitable equations to the Hall-effect–versus–temperature data. The resistivity, Fermi level, and Hall mobility were also found for each sample as a function of temperature. Measurements of the Hall effect and resistivity as a function of pressure were then made at temperatures such that the dependence of ionization energy on pressure could be determined for the *A*, *B*, and *C* levels.

III. EXPERIMENTAL DETAILS

Information about all our samples is summarized in Table I. All samples except 3, 4, and 7 were prepared in this laboratory.[3] Sample 3 was obtained from the MIT Lincoln Laboratory, and 4 and 7 from the General Electric Research Center. The prescription used is essentially the same as that used by Carlson *et al.*[12] It involved a high-temperature diffusion method rather than pulling the crystals from a doped melt.

After the diffusion process, the parallelepipeds were then either lapped to final sample dimensions using 600 and/or 1200 SiC powder or lapped to a thickness of about 0.75 mm and then cut ultrasonically with a Cavitron into a shape having a rectangular parallelepiped body and four narrow arms for the attachment of potential contacts. The electrical contacts to silicon were formed either using an electroless nickel plating[15] or alloying Sb-doped gold spots to the silicon.

The apparatus for generating gas pressures in our laboratory is a commercial two-stage 14-kbar pumping station made by Harwood Engineering with several additions. The pressure in the system is measured using both a Heise bourdon gauge for lower pressures and two manganin gauges whose calibration is traceable to the N.B.S. The output of the manganin gauges is fed into a Foxboro 3 range recorder.

The pressure vessel used for gas pressures to 14 kbar was made from a nonmagnetic Be-Cu alloy and was designed using the engineering information and technique available in the literature.[16,17] The actual design and washer arrangement used are described elsewhere.[3]

Methods for bringing out electrical leads from high-pressure vessels have been discussed extensively in the literature.[18–20] The method adopted here incorporates oil and Epoxy seals and provides a very safe seal. The Epoxy seal is made using Eccobond 104,[21] but with 5–10% AlO_2 added for strength.[22] The procedure for introducing Epoxy into the 3M high-pressure tubing is similar to that of Goree *et al.*[23]

Helium gas invariably leaks through any Epoxy

TABLE I. Characteristics of silicon samples before and after doping with sulfur.

		Conditions before doping			Conditions after doping		
Sample No.	Designation	Starting material[a]	$+1.R_He$ (cm^{-3})[b]	ρ (Ω cm)	$-1/R_He$ (cm^{-3})[c]	ρ (Ω cm)	μ_H (cm^2/V sec)
1	19804-4	Undoped (011)	1.1 E12	1932	6.2 E15	1.1	920
2	19804-5	Undoped (011)	1.2 E12	1935	4.5 E15	1.1	1270
3	226.1	(011)			6.2 E15	0.92	1130
4	CD1162	Undoped			1.7 E16	0.35	1120
5	DC-1.22-16	Boron (111)	1.2 E16	1.4	4.3 E15	1.9	770
6	DC-1.19-16	Boron (111)	1.19 E16	1.5	4.7 E15	1.9	700
7	CD553	p type		~20	8.1 E14	5.8	724
8	DC-1.66-16	Boron (111)	1.66 E16	1.0	2.4 E15	4.2	610
9	DC-9.4-15	Boron (111)	9.4 E15	1.7	1.0 E15	7.8	800
10	DC-1.0-16	Boron (111)	1.0 E16	1.6	4.7 E14	16	810

[a]The numbers in parentheses indicate the plane of the sample that was perpendicular to the magnetic field.

[b]Measured at room temperature with $B=7000$ G. The values are given in a notation such that the number 1.1 E12 is read 1.1×10^{12}.

[c]Measured at room temperature. The values were independent of magnetic field strength between 1 and 10 kG.

seal, and attempts have been made using Epoxy and frozen oil to stop these leaks. These were tried and found inadequate. A simple solution to this problem was found. This consists of placing a short 2-in. head of silicone (1000 cP) oil above the Epoxy on the high-pressure side of the seal. This arrangement forces oil into any channels in the Epoxy and prevents any small gas leaks. Seals made in this way consistently neld helium gas pressure to 13 kbar for several days. However, we found that application of pressures above 8 kbar caused the insulation resistance to break down so that we limited our measurements to pressures below that value.

All silicon samples displayed linear I-V curves passing through the origin. Fields up to ~2 V/cm were applied. Most electrical measurements were made using applied electric fields about two orders of magnitude less than that maximum. The potential drop (PD) was measured as a function of position along the length of a sample for several samples to determine whether or not the diffusion of sulfur into these samples was uniform. The curves of PD versus position were linear to within 0.5%. Carrier concentration variations of about 6% or more would have been obvious, and, in fact, Hall-effect measurements on two different sets of potential leads usually showed less than a 6% difference.

A Hall apparatus[24] was used to make accurate Hall-effect and resistivity measurements from 300 to 80 K. The voltages developed across any of the standard resistors were measured either with a L & N-type K-3 potentiometer using a L & N stabilized dc microvolt indicating amplifier as the null detector or a Keithley 600A electrometer for the higher-resistance samples. The latter instrument was accurate to about ± 2%.

The procedure was to set the temperature at some value and after it became stabilized (in about 5 min) to measure first the Hall effect, always reversing current and field to eliminate unwanted thermomagnetic and resistive voltages, and second, the resistance. Voltages from two sets of leads were measured in most cases and generally agreed to better than 4% for the resistance and 6% for the Hall effect.

The temperature regulation for tne above measurements was accomplished using a model 22 Fisher proportional temperature control. The temperature sensing element was a series of three 100-Ω $\frac{1}{10}$-W Allen-Bradley resistors which were mounted with G.E. 7031 varnish on the base of the sample chamber of the Hall apparatus.[24] The temperature variations at the sample were less than ± 0.01 K. The sample itself was the best indicator of that fact. The absolute value of the temperature using the precalibrated thermocouples which took into account deviations of our thermocouples from those of the N.B.S. was estimated to be in error by < 1%.

Magnetic fields were supplied by a 4-in. Varian magnet. Fields which were reproducible and homogeneous to < 1% with about 0.05% ripple were used for the above Hall-effect measurements. The Hall effect was also measured as a function of magnetic field strength at a few temperatures for several samples and was found independent of field from 100 G to 10 kG with an accuracy of about 1–3% over the whole range and < 0.5% from 2 G to 8 kG. Measurements were usually made at 4480 G.

The Hall effect and resistivity were measured as a function of pressure at various temperatures from 297 to 77.3 K. The desired temperature for these measurements was obtained by the use of one

of several baths for temperatures from 297 to 50 K. The temperature fluctuation at the sample must be kept below a level such that resistance changes because of this fluctuation are small, <1% of the resistance change observed at maximum pressure. For example, in sample 6 at 166 K, $\Delta R/R = -0.096\Delta T$; therefore 1° change in temperature produces a 10% change in resistance, but the pressure induced change of resistance at this temperature is only about 30% in 8 kbar. The temperature in this case must be controlled to ±0.03 K in order to affect the resistance change due to pressure by only 1%. This small variation was achieved by pumping on the various baths and controlling the vapor pressure of the bath with a Cartesian manostat.

After completing all Hall-effect and resistivity measurements, several of our Si(S) samples were analyzed by the Bell & Howell Research Center employing spark source mass spectrometry. In Table II are shown the types and concentrations of several impurities which were detected and the limits of detection for several of our silicon samples.

An important result from these mass spectrographic analyses (MSA) is that for all 12 samples analyzed, sulfur was found to exist in agglomerates.[25] However, the concentration in the agglomerates could not be determined. This agglomeration of sulfur might support the idea that S_2^+ is just two S^+ centers which are close enough together to mutually trap an electron, as suggested by Kravitz.[26] This may also explain the anomalously low room-temperature mobilities which we observe.

Our failure to observe the S^+ (0.612-eV) level is also explainable with the aid of the MSA results which revealed the presence of Mn, Fe, and Zn. Mn and Fe are known to provide deep donor levels at −0.53 and −0.55 eV, respectively, and Zn to provide a deep acceptor level at −0.55 eV. The positions of these levels would prevent appreciable depopulation of the S^+ level by preventing the Fermi level from moving lower than about −0.3 eV.

IV. RESULTS AND DISCUSSION

A. Statistics of Double Donors

From the foregoing it should be evident that sulfur can provide at least two different types of double-donor impurities in silicon. For each type of double donor, two localized states will exist in the energy gap, but they can not be occupied independently, as they cculd if they were due to different single donors.

Champness[27] has developed statistics for the occupation of what he calls the divalent impurity. This center is actually what we refer to as a double donor. It is an easy matter to generalize his results to the case in which there are two types of double donors present as well as shallow donors and acceptors. Thus, when the concentration of holes in the valence band is very small compared to the concentration of electrons in the conduction band, and when all acceptors and all donors having levels much less deep (i.e., much shallower) than those provided by sulfur are ionized at all temperatures of interest, one finds by invoking charge neutrality that the conduction electron concentration n is given by

$$n = N_{sh} - N_{ac} + N_S \frac{(1-f_A)(2-f_D)}{1-f_A+f_A f_D} + N_{S_2} \frac{(1-f_B)(2-f_C)}{1-f_B+f_B f_C}, \tag{1}$$

where N_{sh} is the concentration of shallow donors and N_{ac} the concentration of acceptors. In Eq. (1) it has been assumed that the A and D levels are associated with atomic sulfur of concentration N_S and that the B and C levels are associated with molecular sulfur of concentration N_{S_2}. The justification for these assumptions will become apparent from the discussion of our results. For the upper energy level E_U of a particular type of double donor

$$f_U = \{1 + 2\exp[(E_U - \zeta)/kT]\}^{-1},$$

so that $U = A$ or B. For the lower energy level E_L of a particular type of double donor

$$f_L = \{1 + \tfrac{1}{2}\exp[(E_L - \zeta)/kT]\}^{-1},$$

so that $L = C$ or D. In both f_U and f_L, ζ is the Fermi energy. Since, as we shall see later, our data show no indication of the ionization of level D, we can set $f_D = 1$. Furthermore, even when both S and S_2 centers occur in a given sample, only one of the levels A, B, and C ionizes in a given temperature range because the separations of these levels are large compared to kT. When only one of the levels A, B, and C is ionizing, Eq. (1) reduces to the form[28]

$$\frac{n(n+N_{ac}-N_t^d)}{N_d-(N_{ac}-N_t^d)-n} = \beta_d N_c \exp\left(\frac{E_d}{kT}\right), \tag{2}$$

where $N_c = 2(2\pi m^* kT/h^2)^{3/2}$ is the thermally available number of states per unit volume located at the conduction-band edge taken to be at zero energy, and the approximation $n = N_c \exp(\zeta/kT)$ was used since $|\zeta| > kT$. d stands for A, B, or C depending on which level is ionizing, and quantities associated with each case of ionization are given in Table III. When level C is ionizing, N_{S_2} occurs in N_t^c because level C is the lower of the two levels associated with one of the types of double donors (i.e., S_2). Mathematically this is reflected by the 2 in the $2 - f_C$ factor. It causes the equation for n to have a denominator of $2N_{S_2} + N_S - (N_{ac} - N_{sh}) - n$, which, upon regrouping, takes the form indicated in Eq. (2).

TABLE II. Impurity concentrations in sulfur-doped silicon samples.

Element	Detection limit[a]	Sample number[a,b] 2	3	4	6	8	9
S	0.1	0.34	0.29	0.67	0.78	0.46	0.24
Li	0.1	*ND*	*ND*	*ND*	*ND*	*ND*	*ND*
Mn	0.03	0.078	0.36	0.37	0.051	0.039	0.24
B	0.02	*ND*	*ND*	*ND*	0.02	0.05	0.02
Ni	1.0	*ND*[c]	1	1	*ND*[c]	*ND*[c]	*ND*[c]
Fe	1.0	2.2	20	12	1.9	4.3	12
Cu	0.03	0.37	10	5.4	0.3 to 1.5	4.5	0.46
Zn	0.03	0.14	0.20	2.1	0.23	0.2	0.11
Cr	0.03	0.36	0.40	1.7	0.17 to 4.8	0.26	2.0
O	0.01	41	6.2	52	37	41	29

[a]Units are ppma; 1 ppma $= 10^{-4}$ atomic percent $= 5.0 \times 10^{16}$ atoms/cm^3 in silicon.

[b]Estimated error (see text) is 40–50% when impurity concentration is several time the detection limit. Near the detection limit the error may be 100%.

[c]Detection limit was 3.0 ppma.

B. Hall Effect and Hall Mobility versus Temperature

In order to determine the dependence of the ionization energy of any level on pressure, one must first determine values for certain sample parameters that are independent of pressure. The ionization energy E_I is simply equal to $-E_d$ in Eq. (2) when the zero of energy is taken at the bottom of the conduction band. There is no *a priori* reason that E_I should not be a function of both temperature and pressure. However, analysis of our data indicates a linear pressure dependence of E_I, and we shall assume a linear temperature dependence because the forbidden energy gaps in both Si and Ge vary linearly with temperature. Therefore,

$$-E_d = E_I = E_{I_0} + (\Delta E_I/\Delta T)T + (\Delta E_I/\Delta P)P. \qquad (3)$$

Henceforth, we shall let $\alpha \equiv \Delta E_I/\Delta T$. Our procedure is to measure the resistivity and Hall effect as a function of temperature for each sample and to use the results of these measurements to determine the best values for N_d, $N_{ac} - N_t$, E_{I_0}, and α. The curves obtained by plotting the Hall effect and resistivity versus $10^3/T$ also allow one to see the temperature region over which any particular level is active. Figures 2–4 display $n = (R_H e)^{-1}$ versus $10^3/T$ on semilogarithmic plots. The data on each sample are then used in the nonlinear least-squares-fit program to calculate the unknown parameters which gave the best fit to the data, both for the case in which α is assumed to be equal to zero and for the case $\alpha \neq 0$. The values obtained for the various parameters are given in Table IV.

TABLE III. Quantities associated with each case of ionization.

d	N_d	N_t^d = total concentration of shallower donor levels	β_d
A	N_S	N_{sh}	2
B	N_{S_2}	$N_{sh} + N_S$	2
C	N_{S_2}	$N_{sh} + N_S + N_{S_2}$	$\frac{1}{2}$

The value of $\alpha \neq 0$ obtained by fitting Eq. (2) to the data represents the explicit change of the ionization energy with temperature if, and only if, all the other parameters such as m^* in Eq. (2) are independent, or nearly independent, of temperature. It is known that $(1/m^*)(\Delta m^*/\Delta T) = +4.5 \times 10^{-4}$ K^{-1} for silicon. If this is included in N_c in the above equations, then $\Delta E_I/\Delta T$ decreases by ~2%, which is well within the 20% error deduced for this parameter.

The average values of $\alpha\,(= -\Delta E_d/\Delta T)$ determined for each level are

$$A(S^0 \text{ or } S_2^0): +0.25 \pm 0.05 \text{ meV/K},$$

$$B(S_2^0 \text{ or } S^0): +0.057 \pm 0.012 \text{ meV/K},$$

$$C(S_2^+): -0.61 \pm 0.12 \text{ meV/K}.$$

Several investigators have attributed this explicit dependence of the energy on temperature to an electron-phonon interaction.[29] Actually, no theory has been able to predict the magnitude of this temperature coefficient. Recently, Cheung and Barrie[30] have attempted to deduce the energy shift of

TABLE IV. Least-squares-fit parameters for Si(S) samples.

Sample No.	Center	$E_I = -E_d$ (eV)	$\alpha \equiv \Delta E_I/\Delta T$ (10^{-4} eV/K)	N_d (10^{15} cm^{-3})	$N_{ac} - N_t$ [a] (10^{14} cm^{-3})	Region of fit (K)
2	A	0.10	0	0.75	−0.27	165–50
		0.08	3.3	1.2	−0.19	165–50
3	A	0.11	0	1.3	1.2	165–50
		0.08	2.0	2.5	11	165–50
4	A	0.11	0	4.6	−9.4	165–50
		0.08	2.5	6.5	−2.9	165–50
5	?	0.14	0	3.0	28	300–120
		0.14	1.6	0.58	3.4	300–120
6	B	0.18	0	12	60	300–120
		0.18	0.57	9.5	30	300–120
7	B	0.21	0	1.3	4.0	300–120
		0.22	0.33	1.2	2.8	300–120
2	B	0.19	0	4.2	−7.7	300–165
3	B	0.20	0	5.2	−12	300–165
4	B	0.19	0	16	−55	300–165
8	C	0.32	0	200	−0.012	300–130
		0.36	−5.8	2.9	−0.012	300–130
9	C	0.35	0	86	0.050	300–160
		0.41	−6.4	1.3	0.0038	300–160

[a] N_t identified in text after Eq. (2).

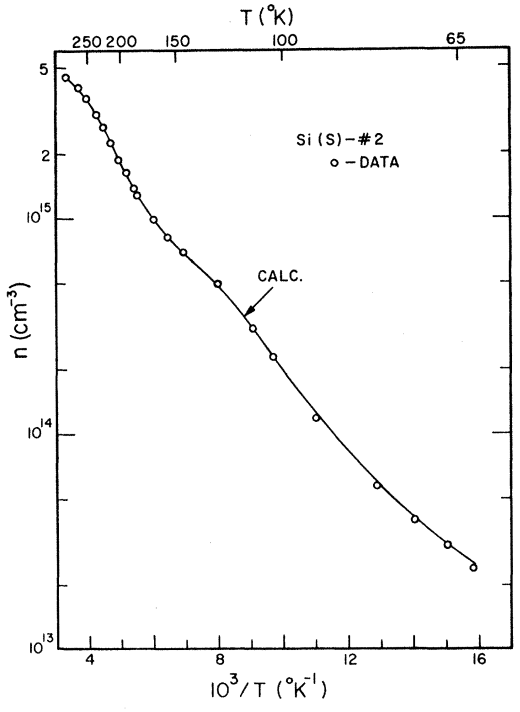

FIG. 2. Carrier concentration as a function of reciprocal temperature for a sample of Si(S). The calculated curve was obtained by fitting Eq. (2) to the data. Above 165 K the B level is ionizing and $E_{I_0} = 0.19$ eV. Below ~165 K level A is ionizing and $E_{I_0} = 0.11$ eV.

several low-lying states for a shallow donor (i.e., P) in silicon by calculating, for example, the energy shift of the $1s(A_1)$ ground state due to its coupling with higher-lying energy states (up to $2P_0$) via the electron-phonon interaction. Their calculated values give the shifts of a particular level at temperature T relative to its position at 0 K. We cannot correlate the shift of the $1s(A_1)$ level with the change of the ionization energy, since we do not know how much the conduction-band edge has shifted relative to its position at $T = 0$ K.

Before discussing the plots of the experimental data and the calculated curves given in Figs. 2–4 we should comment about how the experimentally determined Hall coefficient R_H is actually related to the calculated carrier concentration. Throughout this text it has been assumed that $n = (R_H e)^{-1}$. Actually, we should have written $n = r(R_H e)^{-1}$, where r is a function of the type of band structure, the type of scattering, the crystallographic orientations of the current I and the magnetic induction B, and of the magnitude of B. For either of the extreme cases $\mu B/c \gg 1$ or $\mu B/c \to 0$, the Hall factor r becomes independent of the crystallographic orientation of either I or B. (μ is the mobility of the charge carriers and c is the velocity of light.) For our samples $\mu B/c \leq 0.05$, and the condition $\mu B/c \gg 1$ is not satisfied. If the maximum value of r in the weak-field limit is assumed, then the error introduced into each parameter N_d, $N_{ac} - N_t$, E_{I0}, and $\Delta E_I/\Delta P$

TABLE V. Parameters for Si(S) sample 6 deduced for $r=1.0$ and $r=1.7$.

	N_d (10^{16} cm^{-3})	$N_{ac}-N_{sh}-N_S$ (10^{15} cm^{-3})	E_{I_0} (eV)	$\Delta E_I/\Delta P$ (meV/kbar)
$n=(R_He)^{-1}$	1.16	6.02	0.180	−0.516
$n=1.7\,(R_He)^{-1}$	1.60	5.91	0.182	−0.517

by assuming $r=1.0$ can be found. In the weak-field limit, r may be as large as 1.7 if ionized impurity scattering were the dominant scattering mechanism. Table V shows a comparison of the parameters N_d, $N_{ac}-N_t$, E_{I0}, and $\Delta E/\Delta P$ for $r=1$ and $r=1.7$. The difference in the values of N_d with $r=1$ and $r=1.7$ is about 27% of the second value. Table V also shows that the two values for $N_{ac}-N_{sh}-N_S$ and E_{I_0} are nearly equal, and, therefore, negligible error results in these quantities by choosing $r=1.0$. The most significant point is that even with the two values for N_d different by 27%, the values of the most important parameter $\Delta E_I/\Delta P$ show a negligible difference.

In the most complicated case electrons from the A(0.10-eV) and B(0.19-eV) levels ionized in sequence as the temperature was raised from 50 K. This produces the behavior of sample 2, as shown in Fig. 2. Specifically, the A(0.10-eV) level was

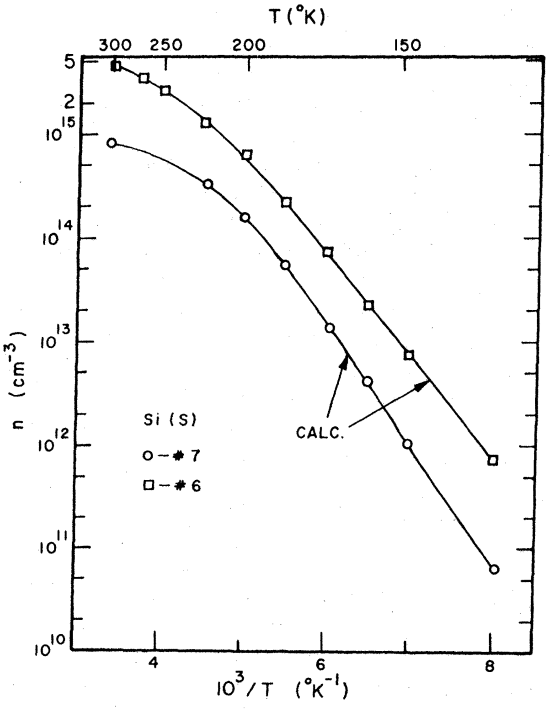

FIG. 3. Carrier concentration as a function of reciprocal temperature for two samples of Si(S). The calculated curves were obtained by fitting Eq. (2) to the data, yielding $E_{I_0}=0.19$ eV.

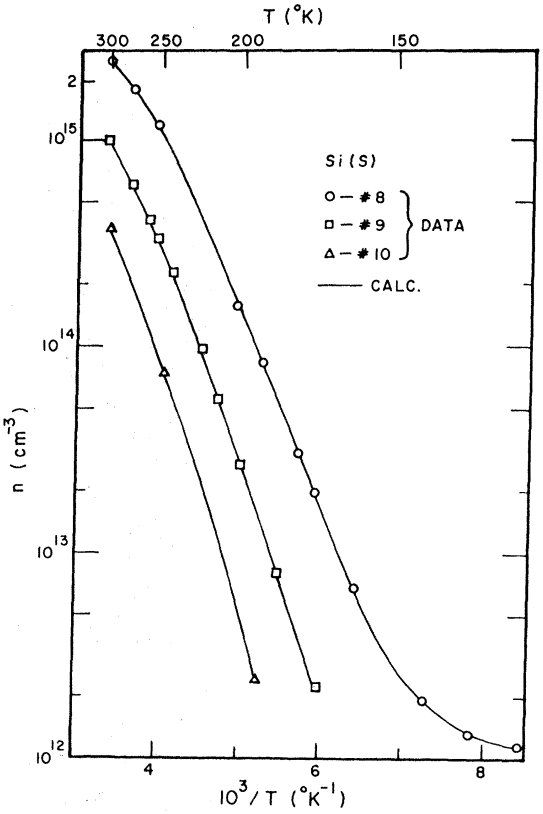

FIG. 4. Carrier concentration as a function of reciprocal temperature for Si(S): 8–10. The calculated curves were obtained by fitting Eq. (2) to the data, yielding $E_{I_0}=0.36$ eV.

ionizing in the temperature range from about 65 up to 165 K. Exhaustion of the A level probably took place near 165 K, and then the B level dominated the Hall effect and resistivity of the sample from 165 to 300 K. By the least-squares fitting of Eq. (2) to the data of samples 2–4 in the two temperature regions (50–165 K) and (300–165 K), we obtained values of the parameters related to the A and B levels, respectively. The calculated fits to data for various samples using these parameters are displayed as solid lines in Figs. 2–4. The parameters found for all the samples by least-squares fitting Eq. (2) to the data are tabulated in Table IV.

Figure 3 shows cases where the B(0.19-eV) level is ionizing over the entire temperature range covered. The curvature near room temperature implies that the level is nearing exhaustion. Values of the parameters for samples 6 and 7 are also tabulated in Table IV.

Figure 4 shows data and the least-squares fit to the data on samples 8 and 9, which are believed to display the S_2^+ level. The two curves appear dif-

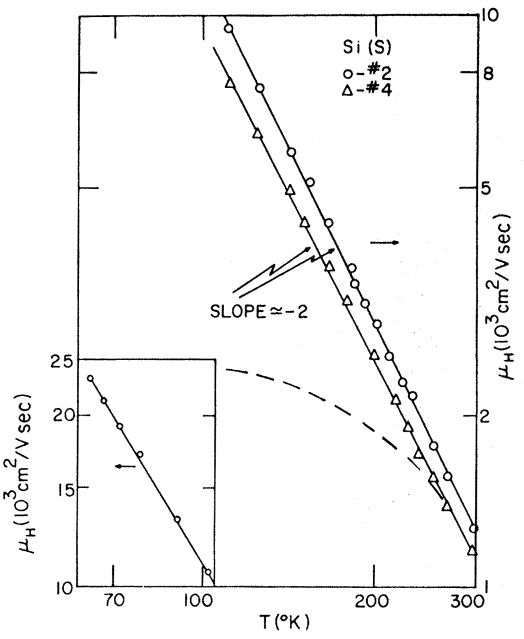

FIG. 5. Dependence of the Hall mobility on temperature for Si(S): 2 and 4.

ferent because $N_{ac} - N_t$ has a different sign in sample 8 than in sample 9, as can be seen in Table IV. For samples 8 and 9 the choice of $\alpha = 0$ would require a concentration N_d of sulfur donors of about 10^{17} cm^{-3}. However, from the MSA and results by Carlson *et al.*[12] it is believed the maximum number of sulfur impurities that can be diffused into silicon is between 3×10^{16} and 4×10^{16} cm^{-3}. Therefore, it seems necessary to take $\alpha \neq 0$ to get a reasonable fit to the data.

Figure 5 displays a log-log plot of the Hall mobility versus temperature for two samples. This behavior was observed in all samples (1–4) in which the starting material was undoped p-type silicon. The mobility can be represented by the empirical relation

$$\mu_H(T) = (1200 \pm 100)\,(T/295)^{-2.1\pm0.2}\ (\mathrm{cm^2/V\,sec}). \quad (4)$$

For these samples the mobility is smaller in magnitude, but has the same dependence on temperature observed[31] for high-purity float-zoned Si between 100 and 320 K. We have been unable to account quantitatively for our observed mobilities in terms of the scattering mechanisms most likely to be important, i.e., lattice,[32] ionized impurity,[33,34] and neutral impurity.[35] Although we have not investigated it in great detail, the addition of a mobility killer mechanism[36] due to space-charge scattering[37] might help to account for our experimental mobilities. (Presumably agglomerations of sulfur would be the mobility killer.)

Samples whose starting material was boron-doped silicon invariably displayed lower room-temperature Hall mobilities than those discussed above. The Hall mobility of sample 6, shown in Fig. 6, is an example of this group. It has a room-temperature Hall mobility of about 700 cm^2/V sec. The high-temperature part of the curve displays a mobility proportional to $T^{-1.6}$. As the temperature is lowered the curve begins to flatten out. It is believed that this occurs because ionized impurity scattering becomes the dominant scattering mechanism at lower temperatures. The solid line in Fig. 6 was calculated by combining an empirical mobility which fits the high-temperature region, namely,

$$\mu_E = 800\,(T/295)^{-1.6}\ (\mathrm{cm^2/V\,sec}), \quad (5)$$

with the mobility limited by ionized impurity scattering[33,34] following the method of Conwell.[38] Conwell's method was actually for obtaining the resultant mobility when the lattice scattering mobility $\mu_L \sim T^{-1.5}$ and the ionized impurity scattering has a simple form. For our calculation the concentration of ionized impurities was taken equal to $n + 2N_{ac}$, where n is the carrier concentration and N_{ac} is the concentration of shallow acceptors. We took $N_{ac} = 1.1\times10^{16}$ cm^{-3} because sample 6 had that acceptor

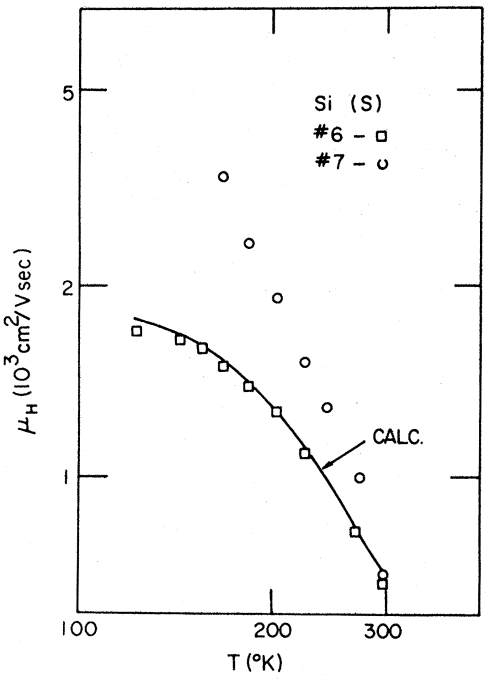

FIG. 6. Dependence of the Hall mobility on temperature for Si(S): 6 and 7. The curve is calculated for a combination of empirical and impurity scattering (see text).

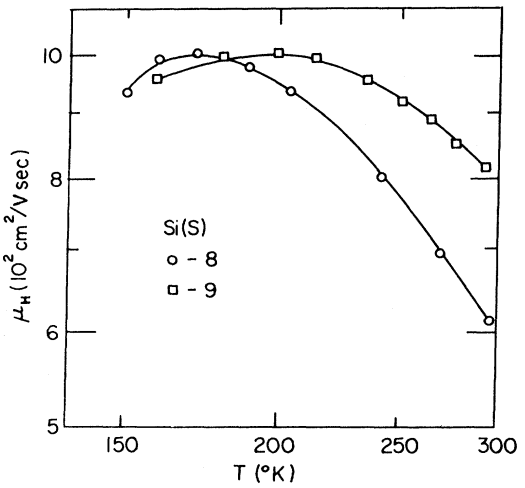

FIG. 7. Dependence of the Hall mobility on temperature for Si(S): 8 and 9.

concentration before sulfur was diffused into it. From Fig. 6 we see that the calculated curve fits the data quite well. Thus we conclude that scattering represented by the empirical relation in Eq. (5) and ionized impurity scattering are the two dominant scattering mechanisms in this sample and in other samples displaying this mobility-versus-temperature relation.

Figure 7 displays the Hall-mobility–versus–temperature data on a log-log plot for samples 8 and 9. The maximum mobility of sample 8 is about 70% above its room-temperature value, while that of sample 9 is only about 25% above its room-temtemperature value. Both samples display negative slopes of about -0.9 ± 0.1 in the high-temperature region, indicating that the Hall mobility is proportional to $T^{-0.9 \pm 0.1}$ for temperatures above 220 K. Both samples display mobilities which attain a maximum of about 1000 cm^2/V sec. We can only guess that the decrease is caused by ionized impurity scattering becoming a dominant scattering mechanism at lower temperature. The relatively small changes observed in sample 9 could be due to a large contribution from neutral impurity scattering, since this mechanism displays only slight temperature dependence through the carrier concentration factor in the expression for the number of neutral donors.[35]

C. Hall Effect and Resistivity versus Pressure

Measurement of the Hall effect as a function of pressure at various temperatures is a direct measure of the dependence of carrier concentration on applied pressure if the change in sample dimensions is taken into account and the scattering mechanism is independent of pressure. The latter will be discussed below.

From the Hall-effect–versus–pressure data we deduced the change of the ionization energy of the ground state of the impurity with pressure for three levels which are introduced by doping silicon with sulfur.

Examples of Hall-effect and resistivity-versus-pressure data are given in Fig. 8, which shows the Hall voltage of sample 8 and the resistivity of sample 5 as functions of hydrostatic pressure. Values obtained with increasing and with decreasing pressure are shown. Note that no hysteresis was found. This was always the case if, and only if, the temperature was kept constant enough.

The most convenient way to handle the pressure data is to normalize the carrier concentration and resistance to the respective values obtained at zero applied pressure. Thus Figs. 9–11 display experimental points $n(P)/n(0)$ versus applied pressure accompanied by the theoretical least-squares fit of Eq. (2) to the data. These calculated fits are displayed as solid lines.

In Sec. III it was determined which of the four levels was changing its degree of ionization drastically in a particular temperature range in each sample. We found that the $A(0.10\text{-eV})$ level was ionizing in samples 2–4 below about 165 K. We can see from Fig. 2 that at 100 K the sample is well within the range where the degree of ionization of the A center is strongly temperature dependent. Having determined the temperature range in which the A level ionizes, we measured the Hall effect and resistivity as a function of hydrostatic pressure in that temperature region. In order to see if $\Delta E_I/\Delta P$ is a function of temperature, data were taken at 90.3 and 77.3 K. Figure 9 shows relevant data for sample 2. The parameters used in Eq. (2) were just those found for sample 2 in the temperature region below 165 K (see Table IV).

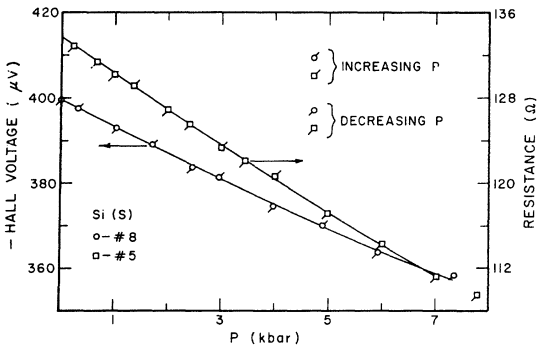

FIG. 8. Hall voltage at 243 K for Si(S): 8 and resistance at 195 K for Si(S): 5, as a function of increasing and decreasing hydrostatic pressure.

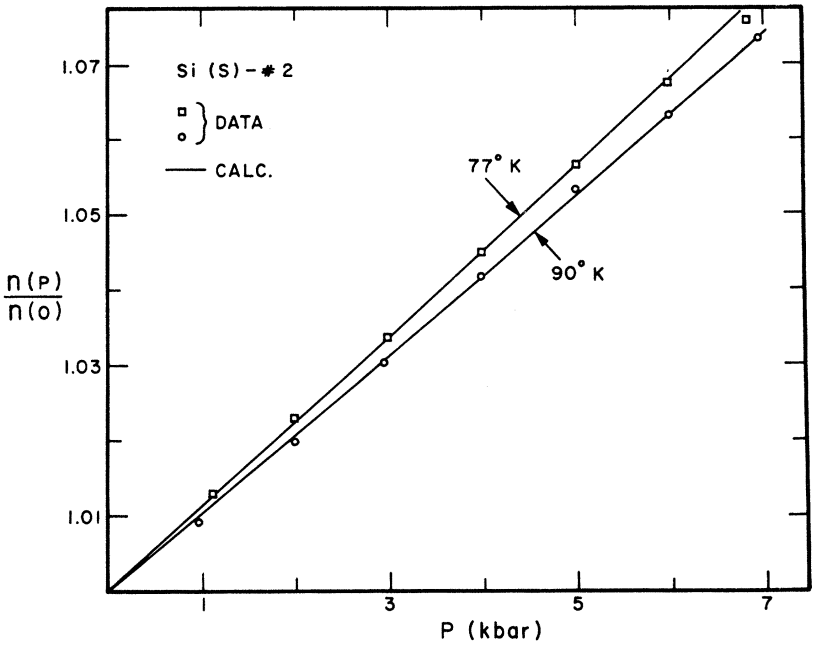

FIG. 9. Dependence of the normalized carrier concentration on applied hydrostatic pressure for the 0.11-eV level at two temperatures. The curves were calculated by employing Eq. (2), with $\Delta E_I/\Delta P = -0.22$ meV/kbar.

In this section we shall analyze the data in two ways. Both ways consist of least-square fitting Eq. (2) to the normalized carrier concentration and thereby determining the $\Delta E_I/\Delta P$ at each temperature for each sample. The first way utilizes the three parameters N_d, $N_{ac}-N_t$, and $E_d(T=0)$ determined from Hall-effect–versus–temperature measurements, and the second way uses four parameters (the fourth being α) which were also determined from the Hall-effect–versus–temperature data. The differences found in the values of $\Delta E_I/\Delta P$ with $\alpha=0$ or $\alpha\neq 0$ are very small.

The B level was found to be ionizing in samples 2–4 at temperatures above 165 K and in samples 6 and 7 over most of the temperature range (120–300 K). The parameters which were calculated using only the Hall-versus-temperature data are listed in Table IV. The solid lines depict the theoretical least-squares fit of either Eq. (2) or (3) with only the parameter $\Delta E_I/\Delta P$ to be fit. Similar results were found for samples 3 and 4.

Figure 10 displays the most complete sets of pressure data at various temperatures for the B (0.19-eV) level of sample 6. Similar results were

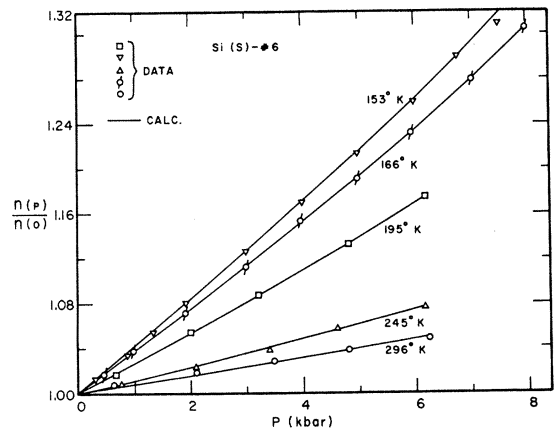

FIG. 10. Dependence of the normalized carrier concentration on applied hydrostatic pressure for the 0.19-eV level of sample 6. The curves were calculated employing Eq. (2), with $\Delta E_I/\Delta P = -0.52$ meV/kbar.

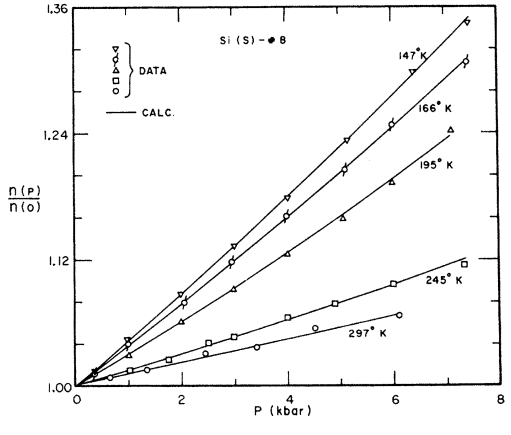

FIG. 11. Dependence of the normalized carrier concentration on hydrostatic pressure for the 0.36-eV level of sample 8. The curves were calculated employing Eq. (2), with $\Delta E_I/\Delta P = -1.1$ meV/bar.

found for sample 7. The values calculated for $\Delta E_I/\Delta P$ with $\alpha = 0$ and $\alpha \neq 0$ are all within 6% of each other. The variation with temperature of $\Delta E_I/\Delta P$ is erratic, and therefore not attributable to an explicit temperature dependence. The room-temperature pressure coefficient is larger in magnitude than those found at lower temperatures. This is probably due to the deeper level, C or S_2^+ (0.36 eV), contributing conduction electrons as the B level reaches exhaustion. This seems probable since the Fermi level has passed through the 0.19-eV level and is at about -0.22 eV at 330 K.

Relative carrier concentration versus pressure at several temperatures for sample 8 are displayed in Fig. 11. Sample 9 gave similar results. The parameters found from the Hall-effect–versus–temperature measurements seemed to give the best results when α was not set equal to zero.

Table VI summarizes the best values for each level of the parameters E_{I_0}, α, and $\Delta E_I/\Delta P$ obtained both when α was set equal to its best value and when α was set equal to zero.

The energy gap ($\Gamma'_{25}-\Delta_1$) of silicon becomes smaller with increasing pressure at a rate of 1.5 meV/kbar. This and other information on the silicon band structure is given in Fig. 12. Therefore, the A (0.105-eV), B (0.19-eV), and C (0.36-eV) levels move toward the valence-band edge with increasing pressure at rates of 1.28, 0.95, and 0.4 meV/kbar, respectively. We notice that the deeper the level is in the energy gap, the smaller is its shift toward the valence-band edge for a given applied pressure.

The Hall-effect and resistivity-versus-pressure data can be combined to yield the dependence of the mobility on pressure. Figure 13 shows a typical example of the normalized mobility plotted as a function of pressure. The total increase in mobility is ~3% in 5 kbar so that $(\Delta n/n\Delta P)_T \approx 4.3 \times 10^{-3}$/kbar. Since the value of the mobility itself cannot be accounted for quantitatively, we shall only remark that such a pressure coefficient could be accounted for at least in part by the effect of pressure on three of the scattering mechanisms which are likely to be involved: lattice, ionized impurity, and neutral impurity scattering.

D. Rubber-Band Effect

In Table VI are listed the pressure coefficients of the ionization energy for the three levels A, B, and C in silicon. It can be seen that the farther the level lies below the conduction band, the larger is the shift toward the conduction-band minima, and the smaller is the shift toward the valence-band edge due to pressure.

An analogy can be made between the energy shifts of each of the sulfur levels and the positional shifts of points on a rubber band which is being stretched. As it is stretched, each point of the rubber band will be displaced with respect to each constrained end by an amount proportional to its original separation from that end. This is, qualitatively but not quantitatively, the way in which the three sulfur levels here considered move with respect to the two band edges as the pressure is changed. For simplicity, we shall say that they exhibit the rubber-band effect.

V. SYMMETRY CONSIDERATIONS FOR MODELS OF SULFUR IN SILICON

The classification of one-electron wave functions for perfect crystals according to their symmetry with respect to the operations of the space group of the crystal[39] is basic. The commonest descrip-

TABLE VI. Best experimental values for E_{I_0}, $\alpha \equiv \Delta E_I/\Delta T$, and $\Delta E_I/\Delta P$ (underlined) and the values of E_{I_0} and $\Delta E_I/\Delta P$ assuming $\alpha = 0$ for Si(S) samples.[a]

Center		A	B	C
Parameter	E_{I_0}[b]	0.109 eV	0.187 eV	0.368 eV
$[E_{I_0}]_{\alpha=0}$ (eV)		0.105±0.015	0.190±0.02	0.36±0.03
$[E_{I_0}]_{\alpha\neq0}$ (eV)		0.08 ±0.015	0.183±0.02	0.38±0.03
α (meV/K)		0.25 ±0.05	0.057±0.012	−0.61±0.12
$[\Delta E_I/\Delta P]_{\alpha\neq0}$ (meV/kbar)		−0.22 ±0.03	−0.55 ±0.05	−1.1 ±0.1
$[\Delta E_I/\Delta P]_{\alpha=0}$ (meV/kbar)		−0.22 ±0.03	−0.54 ±0.05	−1.1 ±0.1

[a]For Si, $\Delta E_{gap}/\Delta T = -0.45$ meV/K. See, for example, H. Brooks, Ref. 29, p. 123. Also $\Delta E_{gap}/\Delta P = 1.5$ meV/kbar; see Ref. 4, Table 8.5, p. 245.
[b]From Ref. 9.

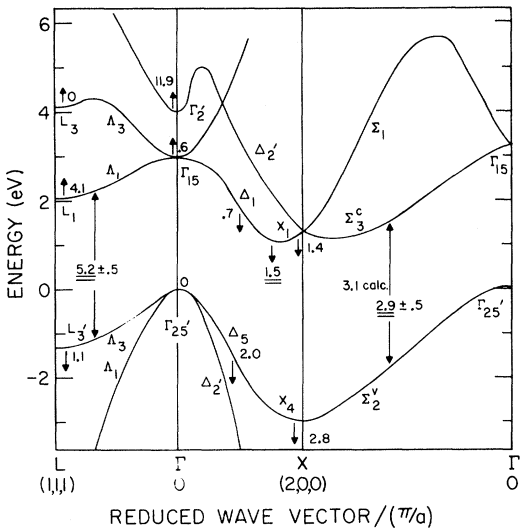

FIG. 12. One-electron band structure for silicon along three symmetry directions, after F. Herman, R. L. Kortum, and C. D. Kuglin, in *Slater Symposium Issue, International Journal of Quantum Chemistry*, edited by Per-Olov Löwdin (Interscience, New York, 1966), p. 381. Short arrows indicate the direction of shift relative to valence-band maximum Γ'_{25} as hydrostatic pressure is applied. The numbers indicate the magnitude of the rates in meV/kbar. The three underlined values are experimental values, from the Zallen and Paul article cited in Ref. 5.

tion of the energy bands in a crystal is provided by plots of the electron energy against $\vec{k}$ for propagation vectors $\vec{k}$ with various special directions in the crystal, each curve or point of special symmetry being labeled with the symmetry of the wave functions corresponding to the subgroup of operations of the space group that leave $\vec{k}$ invariant. Figure 12 shows the familiar representation of the silicon band structure in these terms. The localized wave functions associated with localized impurities or imperfections are similarly characterized by their behavior under the operations in the symmetry group of the imperfect crystal, which consists entirely of rotations. In this section we consider the relevance of these symmetry properties to the rubber-band effect, and supplement the general argument by applications to possible models of sulfur in silicon.

Any localized wave function can be expanded in terms of the complete set of Bloch waves for the perfect crystal – wave functions from all energy bands and all points in the first Brillouin zone in k space. In the case of a shallow donor state produced by a relatively small perturbation, the only Bloch states that appear in the expansion with sizable coefficients are those with energies rather close to that of the impurity state, i.e., those associated with the lowest conduction-band minima. In silicon, the energy surface in k space has six minima; these occur for k vectors $\vec{k}_\Delta$ along the k_x, k_y, or k_z axis, and the associated Bloch functions have Δ_1 symmetry. States with energies near these minima have k vectors near the $\vec{k}_\Delta$, but not necessarily along the axes. Though the corresponding Bloch functions do not, in general, have the Δ_1 symmetry, they may be thought of as associated with Δ_1 valleys in the energy surface. When a substitutional phosphorus atom is introduced into the silicon lattice, a shallow donor level appears about 45 meV below the Δ_1 minima. The corresponding localized wave function can be expressed as a linear combination of Bloch waves in which all components with sizable coefficients have k's near the Δ_1 minima. Alternatively, as in the effective-mass approximation, [1] one can express the wave function as a sum of six terms, each consisting of a Bloch function from the bottom of a valley, with the full Δ_1 symmetry, multiplied by an appropriate localized modulating function.

When stronger perturbations of the potential give rise to deeper levels, the wave functions are more localized, and Bloch waves with a wider range of energy and of $\vec{k}$ contribute importantly to the expansions. The important components may not all be associated with the Δ_1 valleys, and, if the impurity level is well down into the forbidden band, they may include Bloch waves from the valence band. In such cases, effective-mass theory becomes much more complex. In the present context we are interested only in the general understanding provided by symmetry considerations as to what Bloch waves may appear with relatively large coefficients in the expansion of a localized function with given symmetry.

When an impurity state wave function is primarily made up of components from the conduction

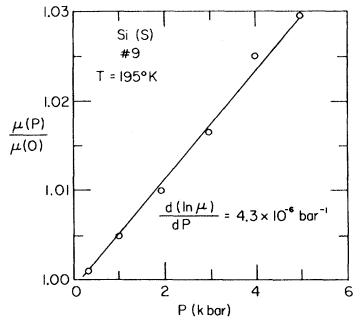

FIG. 13. Dependence of the normalized Hall mobility on hydrostatic pressure for sample 9 at 195 K. The straight-line region ($\lesssim 4$ kbar) yielded a value of $\Delta\mu/\mu\Delta P \simeq 4.3\times10^{-6}$ bar^{-1}.

band, one would expect the energy level to shift only slowly with respect to the conduction band as the pressure is changed; if the function consists mainly of valence-band components, the level should be more or less fixed with respect to the valence band. The intermediate behavior here described as the rubber-band effect is to be expected when both conduction and valence bands make significant contributions to the wave function. To be a bit more precise, one may think of the second-order terms in a perturbation calculation of the impurity state energy as representing its repulsion by the states to which it is coupled by the perturbation, by an amount proportional to the square of the coupling matrix elements and inversely proportional to the energy difference between the states. The rubber-band effect can be expected to result from repulsion of the impurity level by states both above and below it and to be most evident in impurity levels that are strongly coupled by the perturbation both to states low in the conduction band and to states high in the valence band. If there is such coupling, the Bloch functions that represent these states in the unperturbed crystal will appear with sizable coefficients in the expansion of the localized impurity function in terms of Bloch waves. The opposite case of weak coupling and small expansion coefficients is to be expected for Bloch waves with energies widely different from that of the impurity states, or with $\vec{k}$'s for which the perturbation matrix elements are small for reasons of symmetry.

In the Appendix it is shown how to determine what Bloch waves can appear in the expansion of a localized impurity wave function by use of compatibility tables. The Appendix also gives the tables needed in the present case, and some comments on their application. The results are collected in Table VII, in the notation of Ref. 40, for Bloch waves associated with points of type Γ, Σ, Λ, Δ, and L in $\vec{k}$ space.

We consider first the case of the S^+ center, because of its simplicity, even though we have not been able to observe it in the present work. If a single S^{++} ion is substitutional, or occupies one of the interstitial sites in the lattice with T_d symmetry, the total field acting on an additional electron will have T_d symmetry. There are five symmetries possible for localized wave functions in this field. Table VII shows that wave functions of Γ_1 symmetry, which are invariant to all the rotations of the T_d group, can be formed from Bloch waves

TABLE VII. Symmetries of some Bloch functions that can appear in expansions of localized impurity functions.

Symmetry of impurity state	Symmetry of Bloch functions
A. Imperfect crystal with T_d symmetry	
Γ_1	Γ_1, Γ_2', Σ_1, Σ_3, Λ_1, Δ_1, Δ_2', L_1, L_1'
Γ_2	Γ_2, Γ_1', Σ_2, Σ_4, Λ_2, Δ_1', Δ_2, L_2, L_2'
Γ_{12}	Γ_{12}, Γ_{12}', all Σ, Λ_3, Δ_1, Δ_1', Δ_2, Δ_2', L_3, L_3'
Γ_{15}	Γ_{15}, Γ_{25}', all Σ, Λ_1, Λ_3, Δ_1, Δ_2', Δ_5, L_1, L_1', L_3, L_3'
Γ_{25}	Γ_{25}, Γ_{15}', all Σ, Λ_2, Λ_3, Δ_1', Δ_2, Δ_5, L_2, L_2', L_3, L_3'
B. Imperfect crystal with D_{3d} symmetry	
L_1	Γ_1, Γ_{25}', Σ_1, Σ_2, Σ_3, Λ_1, Λ_3, Δ_1, Δ_2', Δ_5, L_1, L_3
L_2	Γ_2, Γ_{15}', Σ_2, Σ_3, Σ_4, Λ_2, Λ_3, Δ_1', Δ_2, Δ_5, L_2, L_3
L_3	Γ_{12}, Γ_{25}', Γ_{15}', all Σ, Λ_1, Λ_2, Λ_3, all Δ, L_1, L_2, L_3
L_1'	Γ_2', Γ_{15}, Σ_1, Σ_3, Σ_4, Λ_1, Λ_3, Δ_1, Δ_2', Δ_5, L_1', L_3'
L_2'	Γ_1', Γ_{25}, Σ_1, Σ_2, Σ_4, Λ_2, Λ_3, Δ_1', Δ_2, Δ_5, L_2', L_3'
L_3'	Γ_{12}', Γ_{25}, Γ_{15}, all Σ, Λ_1, Λ_2, Λ_3, all Δ, L_1', L_2', L_3'
C. Imperfect crystal with C_{3v} symmetry	
Λ_1	Γ_1, Γ_{25}', Γ_2', Γ_{15}, all Σ, Λ_1, Λ_3, Δ_1, Δ_2', Δ_5, L_1, L_1', L_3, L_3'
Λ_2	Γ_2, Γ_{15}', Γ_1', Γ_{25}, all Σ, Λ_2, Λ_3, Δ_1', Δ_2, Δ_5, L_2, L_2', L_3, L_3'
Λ_3	Γ_{12}, Γ_{25}', Γ_{15}', Γ_{12}', Γ_{25}, Γ_{15}, all Σ, all Λ, all Δ, all L
D. Imperfect crystal with C_{2v} Symmetry	
Δ_1	Γ_1, Γ_{12}, Γ_{25}', Γ_2', Γ_{12}', Γ_{15}, all Σ, Λ_1, Λ_3, all Δ, L_1, L_1', L_3, L_3'
Δ_2	Γ_2, Γ_{12}, Γ_{15}', Γ_1', Γ_{12}', Γ_{25}, all Σ, Λ_2, Λ_3, all Δ, L_2, L_2', L_3, L_3'
Δ_3	Γ_{25}', Γ_{15}', Γ_{25}, Γ_{15}, all Σ, Λ_1, Λ_3, all Δ, L_1, L_1', L_3, L_3'
Δ_4	Γ_{25}', Γ_{15}', Γ_{25}, Γ_{15}, all Σ, Λ_2, Λ_3, all Δ, L_2, L_2', L_3, L_3'

with $\vec{k}$'s at and near the bottom of the Δ_1 valleys in the conduction band. It may contain components from the somewhat higher Σ_3 and L_1 valleys in that band (see Fig. 12). It may, indeed, contain components with fairly low energy from every point inside the Brillouin zone except Γ, for which the lowest conduction-band state has the excluded symmetry Γ_{15}; other Bloch states with $\vec{k}$'s near this relatively high portion of the energy surface will, of course, tend to enter only with small coefficients. On the other hand, Bloch waves from the top of the valence band have the excluded symmetry Γ'_{25}, and the other Bloch waves from the upper part of the valence band with symmetries Λ_3, Δ_5, and Σ_2 are likewise excluded. Though valence-band Bloch waves with general $\vec{k}$ are not rigorously excluded by symmetry, it is evident that those with the higher energies will have $\vec{k}$'s near those of excluded waves and will have small coefficients. One thus sees that a Γ_1 state for an impurity site with T_d symmetry would be primarily associated with the conduction band and would tend to move with it as pressure is changed. Inspection of Table VII and Fig. 12 will show that only an impurity state with Γ_{15} symmetry could contain Bloch waves from both the bottom of the conduction band and the top of the valence band and would be expected to exhibit a marked rubber-band effect. The ENDOR study by Ludwig[10] seems to support strongly the idea that the S^+ center is due to a sulfur atom in a T_d site, but his observed value of $g = 2.0054$ indicates that there is no spatial degeneracy in the wave function and thus favors the usually assumed Γ_1 symmetry of the ground state over a Γ_{15} symmetry.

The observations of Ludwig[10] indicate the C center is an S_2^+ center, with the two sulfurs in equivalent positions, presumably rather close together. Two models for this center, both with D_{3d} symmetry, seem worthy of consideration. One is the obvious possibility of two substitutional sulfurs in neighboring positions. There are also interstitial sites with D_{3d} symmetry in the lattice, located half-way from a silicon atom to the next silicon in the direction opposite from that to its nearest neighbor, with its threefold axis passing through these silicons.[41] The silicon atoms nearest to such interstitial sites form a puckered hexagonal ring, each being at a distance that is $\sqrt{\frac{11}{12}}$ times the distance between nearest neighbors. A pair of sulfurs symmetrically arranged about such a center, along the threefold symmetry axis, could each be distant from all silicons by more than the separation of neighboring silicons and would form an imperfection with D_{3d} symmetry. Other possible structures involve considerably greater sulfur-sulfur separations or reduced symmetry. It will be seen later that the assumption of D_{3d} symmetry for the C center is consistent with a simple model for the B center.

Part B of Table VII shows that, if an S_2^{++} ion that reduces the crystal symmetry to D_{3d} binds an electron in a localized state with L_1 or L_3 symmetry, the wave function can contain Bloch waves from both the bottom of the conduction band and the top of valence band; these states would then be expected to show the rubber-band effect. Bloch waves from the lower part of the conduction band would be expected to have little importance in localized states with L'_2 symmetry; a localized state of this type deep in the forbidden band would be associated primarily with the valence band, despite the absence of a Γ'_{25} component. Localized functions with the other symmetries might contain Bloch waves from both bands, but not from the very top of the valence band. The rubber-band effect observed with the C center is thus consistent with a D_{3d} symmetry for the S_2^{++} imperfection and an L_1 or L_3 symmetry of the ground state of a bound electron. Ludwig's conclusion that the state is orbitally nondegenerate would imply that the symmetry is L_1.

It is natural to attempt to interpret the A and B centers as formed by trapping of an additional electron by the C and D centers. If the D center is indeed an S^{++} ion on a T_d site plus an electron in a Γ_1 state, it will produce an average electrostatic potential with T_d symmetry. The observations of Krag *et al.*[9] argue strongly against the identification of the B center as the neutral version of such a D center, but are quite consistent with its being the neutral version of either of the C-center models described above. An S_2^{++} ion forming an imperfection with D_{3d} symmetry, together with a trapped electron in an L_1 state, will produce an average potential with D_{3d} symmetry, will show transitions to p states that vary with stress orientation like those observed by Krag *et al.*, and will, by the argument already applied to the C center, display the rubber-band effect under pressure. There does not, however, appear to be any basis for choice between the models with substitutional or with interstitial sulfurs.

One cannot, however, complete the argument simply by assuming that the A center is the neutral version of the D center. The ground state of an electron trapped by an S^+ center with T_d symmetry would, by the argument applied to the D center, show no rubber-band effect, whereas the A center seems to. Nor can one, on this basis, account for the five levels below the $2p_0$ level attributed to the A center in the analysis of Krag *et al.*[9] It seems possible that there are, in fact, two different types of S^0 centers that contribute to the phenomena attributed to the A center.

Consider, for instance, the possibility that there is an A_1 center, the neutral version of the D cen-

ter, with T_d symmetry, and an A_2 center, a neutral interstitial sulfur at, say, the D_{3d} site described above. Because of lattice absorption, Krag and his associates could not have observed transitions from an A_1-center ground level at about -0.07 eV to high-lying hydrogenic p-like energy levels.[42] It is not unreasonable to assume that the A_1 center is in this region, since the relatively tight binding of the last electron in the D center implies good effective shielding of the core from the final electron added to form an A_1 center and a high ground state for that center. The observed transitions to hydrogenic p levels, which identify a ground level at -0.109 eV, could then be due to an A_2 center. This would account for the rubber-band effect observed by us in the -0.105-eV level and for the presence of the levels near -0.03 eV attributed to the A center by Krag *et al.* The level shown by them near -0.04 eV might, however, really represent a transition from the ground state of the A_1 center to the lowest excited level, which they incorrectly referred to the ground state of the A_2 center because the other transitions of the A_1 center were obscured. This rather speculative interpretation of the "A center" would imply that there is a ground level for the A_1 center, somewhat above the -0.109-eV level, that does not show the rubber-band effect. Our data do not show any clear-cut evidence for the presence of a level with both these properties. On the other hand, our data do not exclude the possibility that A_1 centers are also present in the samples (2–4) which exhibit effects due to A_2 centers. The weak pressure dependence of the A_1 levels could very well be obscured by the rubber-band effect of the A_2 center. Clearly, there is a need for more careful study, both theoretical and experimental, of the A center.

VI. CONCLUSIONS

Hall-effect and resistivity measurements have yielded information about the influence of hydrostatic pressure and temperature on the A–C donor energy levels of sulfur in silicon.

Analysis of Hall-effect–versus–temperature data by least-square fitting charge neutrality equations to the data yielded values for the ionization energies and the explicit parts of the temperature dependences of these levels.

Hall-mobility–versus–temperature data indicate that samples whose starting material was pure float-zoned silicon invariably displayed a Hall mobility which was proportional to $T^{-2.1\pm0.2}$. However, the magnitude of the room-temperature Hall mobility of our samples is 60% of that for pure Si. Our smaller mobilities are possibly due to a mobility "killer" effect originating from the space-charge regions around the agglomerated sulfur.

Samples whose starting material was p type with a carrier concentration between 10^{15} and 10^{16} cm^{-3} displayed Hall-mobility–versus–temperature curves which indicated that scattering by both ionized and neutral impurities had to be combined with an empirical expression for scattering which presumably contains the effects of scattering by both the lattice and sulfur agglomerates.

From Hall-effect–versus–pressure data (up to 8 kbar) at several temperatures between 300 and 77 K, we found that the A–C levels moved with increasing pressure toward the Δ_1 conduction-band edge at rates of 0.22 ± 0.03, 0.55, and 1.1 ± 0.1 meV/kbar, respectively. These levels display a rubber-band effect, in that each level shifts with respect to both conduction- and valence-band edges at a rate that increases with their separation from that edge.

A group-theoretical analysis of the Bloch waves that can enter expansions of localized wave functions of various symmetries, about lattice imperfections with various symmetries, provides a basis for drawing some inferences about the symmetries of the A, B, and C centers from the rubber-band effect. The observed effects are consistent with the idea that the D center is a substitutional or interstitial S^+ at a T_d site, that the C center is an S_2^+ center with D_{3d} symmetry, that the B center is the neutral version of the C center, and that the "A center" is not simply the neutral version of the D center, but may represent, as well, the effects of interstitial sulfur at a D_{3d} site.

ACKNOWLEDGMENTS

We are indebted to Dr. Ludwig of the General Electric Co. and Dr. Krag of the MIT Lincoln Laboratory for supplying some material, and to Miss L. Roth and Professor H. J. Yearian for cutting and orienting several of the crystals. We would also like to thank Dr. J. Cavanagh for his assistance in setting up and debugging the computer programs used in the numerical calculations. We are grateful to Dr. J. Chroboczek and Leif Halbo for their discussions concerning experimental details.

APPENDIX: SYMMETRY CONSIDERATIONS FOR SPECIAL MODELS OF SULFUR IN SILICON

General Discussion

Introduction of a localized imperfection into the silicon crystal removes the translational symmetry of the system and some of the rotational symmetry. If the imperfection has a center of symmetry at one of the nuclei, as when a nuclear charge is changed, that nucleus is distinguished from all others, and all symmetry operations of the original space group O_h^7 that move this nucleus are destroyed; this leaves

only the point group T_d of rotations (proper and improper) about this particular nucleus. The symmetry group of the imperfect crystal then consists of the subgroup of this T_d group to which the imperfection itself is invariant. An imperfection with center of symmetry midway between adjacent silicon atoms (such as would be produced by equal changes in the nuclear charges of these two atoms) would remove all symmetry operations of the original group except a group D_{3d} of rotations about this point, and the symmetry operations of the imperfect crystal would include only the operations of this D_{3d} group to which the imperfection is invariant. In any case, the symmetry group of the imperfect crystal is some subgroup G_I of the group of all rotations O_h that appear in O_h^7. The localized wave functions that describe states of an electron bound to the imperfection can be chosen to be basis functions for some irreducible representation γ_i of G_I, and will necessarily be such unless there is some accidental degeneracy of energy levels.

The expansion of each localized function will contain essentially all Bloch waves that can be employed in the construction of a corresponding basis function for the representation γ_i of G_I; vanishing of the expansion coefficient for any such Bloch wave can be regarded as "accidental," since it arises from no symmetry property of the Bloch wave that assures its orthogonality to the localized function and thus its absence from the expansion. It will be shown that any Bloch wave $\Psi(\vec{k};\vec{r})$ with a "general" $\vec{k}$ [such that all operations of the point group G_I carry $\vec{k}$ into a different orientation and $\Psi(\vec{k};\vec{r})$ into a different function] may be present in the expansion of the basis functions for any irreducible representation of G_I. It will appear, however, that if $\vec{k}$ ends on some special symmetry point, line, or plane in $\vec{k}$ space, and is therefore invariant to one or more of the operations of G_I, then $\Psi(\vec{k};\vec{r})$ may be absent from these expansions for reasons of symmetry; nearby $\vec{k}$ will occur only with small coefficients. If these special $\vec{k}$'s are those of band edge functions, the presence of these band edges will have little effect on the nature of the localized wave function, or, as was argued in Sec. V, on the change of its energy with change in magnitude of the perturbing potential.

Figure 12 presents the silicon energy-band structure in terms of plots of $E(\vec{k})$ for special directions of $\vec{k}$, each labeled with the symbol of the irreducible representation of the group $\mathfrak{K}(\vec{k})$ (the subgroup of operations in O_h^7 that leaves $\vec{k}$ invariant) to which the Bloch wave belongs. In the case of all interior points of the Brillouin zone and also the surface points of types S, U, K, L, and Q, the Bloch-wave basis also bases of irreducible representations, designated by the same symbols, of point groups $G_0(\vec{k})$ consisting of the rotations that appear in the corresponding $\mathfrak{K}(\vec{k})$.[43] We here restrict our attention to such cases.

TABLE VIII. $G_I(\vec{k})$ and $G_0(\vec{k})$, for various G_I and $\vec{k}$.

$\vec{k}$ =	$\vec{k}_\Gamma$	$\vec{k}_\Sigma$	$\vec{k}_\Lambda$	$\vec{k}_\Delta$	$\vec{k}_L$
$G_0(\vec{k})$ =	O_h	C_{2v}	C_{3v}	C_{4v}	D_{3d}
G_I			$G_I(\vec{k})$		
T_d	T_d	C_s	C_{3v}	C_{2v}	C_{3v}
D_{3d}	D_{3d}	C_s or C_2	C_{3v} or C_s	C_s	C_{2h}
C_{3v}	C_{3v}	C_s or E	C_{3v} or C_s	C_s	C_{3v} or C_s
C_{2v}	C_{2v}	C_s or E	C_s	C_{2v} or E	C_s

We have now to determine in what cases Bloch waves $\Psi(\vec{k};\vec{r})$ that belong to a given irreducible representation β_j of $G_0(\vec{k})$ will be absent, for reasons of symmetry, from the expansions of a set of localized functions that form a basis for the irreducible representation γ_i of G_I. Let $G_I(\vec{k})$ be the point group consisting of all rotations that belong to both G_I and $G_0(\vec{k})$. Then the Bloch-wave basis functions for β_j can be used to form bases for irreducible representations of $G_I(\vec{k})$, as can the localized basis functions for γ_i. If in the two cases one obtains bases for any one representation of $G_I(\vec{k})$, corresponding functions from the bases will not be orthogonal by reasons of symmetry, and one must expect at least one of the $\Psi(\vec{k};\vec{r})$ to be present in the expansion of at least one of the localized bases of γ_i. In other words, Bloch waves with β_j symmetry will appear in expansions of localized functions of γ_i symmetry if β_j and γ_i are both compatible with any irreducible basis of their common subgroup $G_I(\vec{k})$.

If $\vec{k}$ is a "general" $\vec{k}$ with respect to the point group G_I, $G_I(\vec{k})$ will contain only the identity; from this it follows that $\Psi(\vec{k};\vec{r})$ may appear in the expansion of any basis function of any irreducible representation γ_i, as was noted above.

Application to Sulfur in Silicon

Table VIII gives the forms of $G_0(\vec{k})$, for the several choices of G_I considered here, and for various choices of $\vec{k}$. It will be noted that there are three cases in which $G_0(\vec{k})$ and G_I are of the same form (D_{3d}, C_{3v}, C_{2v}) but consist of physically different rotations, so that their common subgroup $G_I(\vec{k})$ is smaller and may include only the identity. It will also be noted that $\vec{k}$ that are equivalent with respect to the perfect crystal may not be equivalent with respect to the imperfect crystal, so that there are alternative forms of $G_I(\vec{k})$. In such cases some but not all of the $\Psi(\vec{k};\vec{r})$ for "equivalent" $\vec{k}$ can appear in the expansion of an impurity function belonging to the given G_I.

Table IX contains all compatibility tables needed in the present work, where one has to consider only groups of rotations (proper and improper) contained in O_h. The notation is that of Ref. 40, with a few obvious extensions.[44] Some of the simpler groups appear in connection with several different values of $\vec{k}$; for instance, C_s may be associated with $\vec{k}_\Sigma$, $\vec{k}_\Lambda$, $\vec{k}_\Delta$, or $\vec{k}_L$, and C_{2v} with $\vec{k}_\Sigma$ or $\vec{k}_\Delta$. In such cases Table IX shows a single symbol (Σ or Δ, in these cases) consistently throughout, to simplify the comparison of compatibilities. The trivial compatibility tables that apply when $G_I(\vec{k})$ is the same as G_I, $G_0(\vec{k})$, or E have not been included in Table IX.

In applying these tables to the deduction of Table VII, one fixes attention on a particular G_I and considers in turn the various $\vec{k}$. Table VIII gives the corresponding $G_0(\vec{k})$ and $G_I(\vec{k})$. In one of the sections of Table IX one can then find, to the left of the vertical line, a column listing the irreducible representations of G_I; in the same section of the table there is also a column listing the compatible representations of $G_I(\vec{k})$. Similarly, to the left of the vertical line in a section of Table IX (not necessarily the one referred to in the preceding sentence) there will be found a list of the irreducible representations of $G_0(\vec{k})$, and, in that same section, a list of the compatible representations of $G_I(\vec{k})$. Comparing the two pairs of columns, one can see which representations of G_I and $G_0(\vec{k})$ are compatible with any single representation of $G_I(\vec{k})$.

As a complex example that illustrates many points, consider an imperfection that reduces the crystal symmetry to $G_I = D_{3d}$, and consider $\vec{k} = \vec{k}_\Lambda$. Table VIII shows that the group of $\vec{k}_\Lambda$ in the pure crystal is $G_0(\vec{k}_\Lambda) = C_{3v}$ and that $G_I(\vec{k}_\Lambda)$ is C_{3v} for some $\vec{k}_\Lambda$ and C_s for other $\vec{k}_\Lambda$. For $\vec{k}_\Lambda$ of the first type, $G_0(\vec{k}_\Lambda)$ and $G_I(\vec{k}_\Lambda)$ are identical: The imperfection does not reduce the set of rotations that leaves these $\vec{k}_\Lambda$ invariant. The second section of Table IX shows that localized impurity states with L_3 symmetry (for example) yield only a Λ_3 representation of $G_I(\vec{k}_\Lambda) = C_{3v}$, which is also a Λ_3 representation of $G_0(\vec{k}_\Lambda)$. It follows that Bloch waves with k_Λ of the first type can appear in the expansion of localized impurity states with L_3 symmetry only if they have Λ_3 symmetry. For $\vec{k}_\Lambda$ of the second type the imperfection reduces the group of the $\vec{k}$ to C_s. The second part of Table IX shows that impurity wave functions with L_3 symmetry can yield Σ_1 and Σ_2 representations of C_s. (Since the vector in question is $\vec{k}_\Lambda$, one might prefer to use the symbols Λ_1 and Λ_2, but this does not affect use of the table.) The same section of Table IX also shows that Σ_1 and Σ_2 representations of C_s are compatible with all (Λ_1, Λ_2, Λ_3) representations of the group of $\vec{k}_\Lambda$. It follows that all Bloch waves with this second type of $\vec{k}_\Lambda$ can enter expansions of L_3 impurity states. This accounts for the appearance of all Λ's in the third line of part B of Table VII.

TABLE IX. Compatibility tables used in the present work.

O_h	T_d	D_{3d}	C_{3v}	C_{2v}	C_s
Γ_1	Γ_1	L_1	Λ_1	Δ_1	Σ_1
Γ_2	Γ_2	L_2	Λ_2	Δ_2	Σ_2
Γ_{12}	Γ_{12}	L_3	Λ_3	$\Delta_1+\Delta_2$	$\Sigma_1+\Sigma_2$
Γ'_{25}	Γ_{15}	L_1+L_3	$\Lambda_1+\Lambda_3$	$\Delta_1+\Delta_3+\Delta_4$	$2\Sigma_1+\Sigma_2$
Γ'_{15}	Γ_{25}	L_2+L_3	$\Lambda_2+\Lambda_3$	$\Delta_2+\Delta_3+\Delta_4$	$\Sigma_1+2\Sigma_2$
Γ'_1	Γ_2	L'_2	Λ_2	Δ_2	Σ_2
Γ'_2	Γ_1	L'_1	Λ_1	Δ_1	Σ_1
Γ'_{12}	Γ_{12}	L'_3	Λ_3	$\Delta_1+\Delta_2$	$\Sigma_1+\Sigma_2$
Γ_{25}	Γ_{25}	$L'_2+L'_3$	$\Lambda_2+\Lambda_3$	$\Delta_2+\Delta_3+\Delta_4$	$\Sigma_1+2\Sigma_2$
Γ_{15}	Γ_{15}	$L'_1+L'_3$	$\Lambda_1+\Lambda_3$	$\Delta_1+\Delta_3+\Delta_4$	$2\Sigma_1+\Sigma_2$

D_{3d}	C_{3v}	C_{2h}	C_2	C_s
L_1	Λ_1	L_1	Σ_1	Σ_1
L_2	Λ_2	L_2	Σ_2	Σ_2
L_3	Λ_3	L_1+L_2	$\Sigma_1+\Sigma_2$	$\Sigma_1+\Sigma_2$
L'_1	Λ_1	L_4	Σ_2	Σ_1
L'_2	Λ_2	L_3	Σ_1	Σ_2
L'_3	Λ_3	L_3+L_4	$\Sigma_1+\Sigma_2$	$\Sigma_1+\Sigma_2$

C_{4v}	C_{2v}	C_s	C_{2v}	C_2	C_s
Δ_1, Δ'_2	Δ_1	Σ_1	Δ_1	Σ_1	Σ_1
Δ'_1, Δ_2	Δ_2	Σ_2	Δ_2	Σ_1	Σ_2
Δ_5	$\Delta_3+\Delta_4$	$\Sigma_1+\Sigma_2$	Δ_3	Σ_2	Σ_1
			Δ_4	Σ_2	Σ_2

†Work supported by the U. S. Army Research Office and the Advanced Research Projects Agency. The article is based in part on a thesis presented to Purdue University by D. L. Camphausen in partial fulfillment of the requirements for the Ph. D. degree, 1969.

*Present address: Gordon McKay Research Center, Harvard University, Cambridge, Mass.

[1]W. Kohn, in *Solid State Physics*, edited by F. Seitz and D. Turnbull (Academic, New York, 1956), Vol. 5, p. 257; W. Kohn and J. M. Luttinger, Phys. Rev. 98, 915 (1955).

[2]G. W. Ludwig and H. H. Woodbury, in *Solid State Physics*, edited by F. Seitz and D. Turnbull (Academic, New York, 1962), Vol. 13, p. 243, and references quoted therein.

[3]D. L. Camphausen, Ph. D. thesis, Purdue University, 1969 (unpublished).

[4]W. Paul and D. M. Warschauer, *Solids Under Pressure* (McGraw-Hill, New York, 1963), p. 179, and references quoted therein.

[5]R. Zallen and W. Paul, Phys. Rev. 155, 703 (1967), and references quoted therein; A. Sagar and R. C. Miller, J. Appl. Phys. 32, 2073 (1961).

[6]See Refs. 26, 42, and 43 quoted in Ref. 4 above.

[7]See, for example, W. Paul, in *Proceedings of the Ninth International Conference on the Physics of Semi-*

conductors, (Nauka Publishing House, Leningrad, 1968), Vol. 1, p. 16; and references contained therein.

[8]G. A. Peterson, in *Proceedings of the International Conference on the Physics of Semiconductors*, (Dunod, Paris, 1964), p. 771; H. Kaplan, J. Phys. Chem. Solids 24, 1593 (1963); T. Shimizu, Phys. Letters 15, 297 (1965).

[9]W. E. Krag, W. H. Kleiner, H. J. Zeiger, and S. Fischler, J. Phys. Soc. Japan Suppl. 21, 230 (1966).

[10]G. W. Ludwig, Phys. Rev. 137, A1520 (1965).

[11]Ludwig attributed this value to work of Kravitz and Paul, then unpublished. However, these authors state that the energy of the S^+ level is not actually -0.52 eV, but is probably closer to -0.59 eV which corresponds better with the optically determined -0.6116 eV of Krag *et al.* See L. C. Kravitz, Harvard University, Technical Report No. HP-9, Division of Engineering and Applied Physics, 1963 (unpublished).

[12]R. O. Carlson, R. N. Hall, and E. M. Pell, J. Phys. Chem. Solids 8, 81 (1959).

[13]W. E. Krag and H. J. Zeiger, Phys. Rev. Letters 8, 485 (1962).

[14]See, for example, *Handbook of Chemistry and Physics*, edited by C. D. Hodgman, (Chemical Rubber Publishing Co., Cleveland, Ohio, 1966–1967), 47th ed., p. E65.

[15]M. V. Sullivan and J. H. Eigler, J. Electrochem. Soc. 104, 226 (1957).

[16]W. Paul, G. B. Benedek, and D. M. Warschauer, Rev. Sci. Instr. 30, 874 (1959).

[17]E. W. Comings, *High Pressure Technology* (McGraw-Hill, New York, 1956), p. 160.

[18]M. G. Craford, thesis, University of Illinois (unpublished).

[19]R. H. Cornish and A. L. Ruoff, Rev. Sci. Instr. 32, 639 (1961).

[20]W. S. Goree, B. McDowell, and T. A. Scott, Rev. Sci. Instr. 36, 99 (1963), and references quoted therein.

[21]Purchased from Emerson and Cuming, Inc., Canton, Mass.

[22]L. A. Davis, R. B. Gordon, J. K. Tien, and J. R. Vaisnys, Rev. Sci. Instr. 35, 368 (1964).

[23]Taken from procedure described in Ref. 20.

[24]R. W. Ure, Jr., Rev. Sci. Instr. 28, 836 (1957).

[25]A. J. Socha and E. M. Masumoto (private communication) of Bell and Howell Research Center carried out the analytical investigation by MSA.

[26]L. C. Kravitz, quoted in Ref. 11.

[27]C. H. Champness, Proc. Phys. Soc. (London) B69, 1335 (1956).

[28]J. H. DeBoer and W. Ch. Van Geel, Physica 2, 286 (1935).

[29]For example, see H. Brooks, in *Advances in Electronics and Electron Physics*, edited by L. Marton (Academic, New York, 1955), Vol. VII, p. 118, Refs. 57–59.

[30]C. Y. Cheung and R. Barrie, Can. J. Phys. 45, 1421 (1967).

[31]J. Messier and J. M. Flores, J. Phys. Chem. Solids 24, 1539 (1963).

[32]C. Herring, Bell System Tech. J. 34, 237 (1955); D. Long, Phys. Rev. 120, 2024 (1960), and references contained therein.

[33]E. M. Conwell and V. F. Weisskopf, Phys. Rev. 77, 388 (1950).

[34]H. Brooks, Phys. Rev. 83, 879 (1951); see also Ref. 29, p. 156; C. Herring (unpublished); R. B. Dingle, Phil. Mag. 46, 831 (1955); F. J. Blatt, in *Solid State Physics*, edited by F. Seitz and D. Turnbull (Academic, New York, 1957), Vol. 4, p. 199.

[35]C. Erginsoy, Phys. Rev. 79, 1013 (1950); N. Sclar, *ibid.* 104, 1559 (1956).

[36]L. R. Weisberg, J. Appl. Phys. 33, 1817 (1962).

[37]B. R. Gossick, J. Appl. Phys. 30, 1214 (1959).

[38]E. M. Conwell, Proc. Inst. Radio Engrs. 40, 1327 (1952).

[39]See, for example, F. Seitz, Ann. Math. 37, 17 (1936); L. P. Bouckaert, R. Smoluchowski, and E. Wigner, Phys. Rev. 50, 58 (1936).

[40]The notation used throughout the text is that used by Koster and adopted from earlier works which he cites. See G. F. Koster, in *Solid State Physics*, edited by F. Seitz and D. Turnbull (Academic, New York, 1957), Vol. 5, p. 173.

[41]K. Weiser, Phys. Rev. 126, 1427 (1962).

[42]W. E. Krag (private communication).

[43]See Ref. 40, pp. 231–233, for an indication of the method of constructing the irreducible representations of the $\mathfrak{K}(\vec{k})$ from those of the $G_0(\vec{k})$, for the same basis functions.

[44]In deducing compatibility tables from the character tables of Ref. 40, it is important to keep in mind the physical significance of the group operations, since reflections denoted by σ_v in one table may appear as σ_h or σ_d in another. Much of the largest section of Table VIII follows from tables given by R. H. Parmenter, Phys. Rev. 100, 573 (1955).